Cellular and Molecular Biology
E-ISSN : 1165-158X / P-ISSN : 0145-5680
www.cellmolbiol.org

The effect of Iodine-125 radioactive particle stent with doxorubicin-loaded nano-tetrahedrons combined with transarterial chemoembolization on survival and prognosis of patients with cholangiocarcinoma

Gaobo Wang, Guowei Ye, Xugao Chen, Zhong Ji, Lingtong Wu, Biao Liu*

Department of Radiology, Lishui People's Hospital, Lishui, 323000, Zhejiang Province, China

ARTICLE INFO

Original paper

Article history:
Received: July 14, 2022
Accepted: August 23, 2022
Published: August 31, 2022

Keywords:

doxorubicin-loaded DNA nano-tetrahedrons, I-125 radioactive particle stent, TACE, cholangiocarcinoma, the five-year survival rate

ABSTRACT

This study was to analyze the application of doxorubicin-loaded DNA nano-tetrahedral Iodine-125 (I-125) radioactive particle stent (doxorubicin-loaded I-125 stent) combined with transarterial chemoembolization (TACE) in improving the prognosis of patients with cholangiocarcinoma (CC). The doxorubicin-loaded DNA nano-tetrahedrons were constructed, the preparation plan was optimized, and the toxicity test was performed. The prepared doxorubicin-loaded DNA nano-tetrahedrons were applied to 85 cases in the K1 group (doxorubicin-loaded I-125 + TACE), 85 cases in the K2 group (doxorubicin-loaded I-125), and 85 cases in K3 group (TACE). It was found that the optimal initial concentration of doxorubicin for the preparation of DNA-loaded nano-tetrahedrons was 200 μmol, and the optimal reaction time was 7 hours. The serum total bilirubin (TBIL) level in the K1 group at 30 days after operation was lower than that in the K2 and K3 groups at 7, 14 and 21 days. ($P< 0.05$). The alkaline phosphatase (ALP) level in the K1 group was lower in contrast to that in the other two groups at 7, 14, and 21 days after surgery ($P< 0.05$); and the five-year survival rate of patients in the K1 group was greater in contrast to the rate in K2 and K3 groups ($P< 0.05$). In short, the implantation of a doxorubicin-loaded I-125 stent combined with TACE could effectively improve the five-year survival rate of patients with CC and improve the prognosis effect of the patients.

Doi: http://dx.doi.org/10.14715/cmb/2022.68.8.24

Introduction

CC refers to a malignant tumor of the bile duct from the extrahepatic bile duct, including the hilar area to the lower end of the common bile duct, and is closely related to bile duct stones, clonorchis, and cholangitis (1). Generally speaking, CC patients have no special symptoms in the early stage. As the disease progresses, they may experience jaundice, clay-like stools, dark urine, waist and abdomen pain, elevated body temperature, vomiting, loss of appetite, and weight loss (2,3). Currently, the most effective clinical treatment for CC is surgical resection, which mainly includes radical surgery and palliative surgery. In addition, chemotherapy, radiotherapy, targeted therapy, and bile drainage can also be used to treat CC, but the effect needs to be improved (4). TACE is to connect a special catheter and other equipment to the relevant part of the lesion through the blood vessel. Firstly, the contrast agent is injected for angiography to understand the anatomical changes and pathological changes in the lesion area, then a catheter is inserted into the blood vessel of the tumor, and the chemotherapeutics that can kill tumor cells and embolism that can block the blood supply of the tumor are injected to kill the tumor eventually (5,6). This intervention is a kind of minimally invasive treatment without surgery and general anesthesia, and the wound to the patient is only about 2 mm, which is suitable for most organ solid tumors (7). Therefore, TACE was adopted in this study for the interventional treatment of CC patients.

In addition, I-125 radioactive particles are also called particle knives. It is a new tumor method that complements the defects of surgery and radiotherapy and chemotherapy in the international medical community. It has small trauma, accurate bullseye, low-dose continuous gamma radiation irradiation, and no pollution (8). Radioactive implantation of I-125 radioactive seeds belongs to the category of brachytherapy, and I-125 can be directly implanted into the tumor tissue under the image-guided percutaneous puncture to perform radiation therapy on the tumor (9,10). In recent years, nanotechnology has been widely used in the field of biomedicine. Nanomaterials themselves have relatively specific properties, including large specific surface area, high surface catalytic activity, and surface modification, which can provide a good material basis for the construction of nano drug delivery systems (11,12). There are many kinds of commonly used nano-drug delivery systems, such as plastids, micelles, and carbon nanotubes, all of which have different degrees of drawbacks. For example, the connection of liposome cargo molecules and nano-carriers is non-specific, which greatly reduces the role of

* Corresponding author. Email: liubiao2022@yandex.com

drugs under physiological conditions (13). DNA tetrahedron is a three-dimensional DNA nanostructure composed of four strands, and its tolerance to specific nucleases and non-specific nucleases is much better than that of ordinary linear DNA. Therefore, a DNA-loaded tetrahedral drug delivery system was constructed in this study for CC patient for treatment research (14).

In summary, the doxorubicin-loaded DNA nano-tetrahedrons were constructed using four DNA strands, the preparation protocol was optimized, and a toxicity experiment was performed. Next, the construction nano-tetrahedrons were applied to the clinical treatment of 255 extrahepatic CC patients to comprehensively evaluate the application value of doxorubicin-loaded I-125 combined with TACE in improving the prognosis of CC patients.

Materials and Methods

Research objects and grouping

255 extrahepatic CC patients who were admitted to the Lishui People's Hospital from February 10, 2019 to May 16, 2020 were selected as the research objects, including 68 males and 46 females aged 20 - 71 years old. According to different treatment options, the patients were divided into a K1 group (doxorubicin-loaded I-125 + TACE), a K2 group (doxorubicin-loaded I-125), and a K3 group (TACE), with 85 cases in each group. The study had been approved by the Medical Ethics Committee of Lishui People's Hospital, and the patients and their families understood the situation of the study and signed the informed consent forms.

The inclusion criteria were defined as follows: patients diagnosed with CC; patients who did not undergo surgery, radiotherapy, or chemotherapy during treatment and follow-up; patients who had understood the experiment and signed the informed consent; and patients with complete basic data and imaging data.

The exclusion criteria were defined as follows: patients with intrahepatic tumors; patients with psychiatric diseases; patients who were not reviewed in our hospital after treatment; patients who withdrew from the experiment due to personal reasons; and patients who refused surgery.

Construction and optimization of DNA nano-tetrahedral drug delivery system

The specific steps were as follows. The four DNA strands were separated into equimolar and placed in a mixed buffer of 10 mmol of Tris and 1 mmol of ethylenediaminetetraacetic acid (EDTA), which was allowed to react at 95°C for 3 minutes. Then, it was cooled in ice water to obtain DNA Nano-tetrahedron, which was mixed with doxorubicin. The mixed solution was incubated in the dark at room temperature and centrifuged at 10,000 rpm for 8 minutes to obtain the supernatant and dark red precipitate. The supernatant was adopted to measure the concentration of doxorubicin, and the dark red precipitate was prepared into a 100 μmol of stock solution using 10 mmol of Tris and 1 mmol of EDTA.

The optimization experiment was performed with the following procedures. The DNA nanotetrahedrons and different concentrations (10, 50, 100, 150, and 200 μmol) of doxorubicin were mixed to react, and centrifuged at 10,000 rpm for 20 minutes. Calculating the concentration of doxorubicin in the supernatant can obtain the actual concentration of doxorubicin loaded in the DNA tetrahedron. The DNA nanotetrahedron was mixed with adriamycin. The concentrations of adriamycin under different reaction times (1, 3, 5, 7, and 9 hours) were calculated to obtain the best reaction time.

Characteristics of DNA nano-tetrahedron

The Methyl Thiazolyl Tetrazolium (MTT) was used to detect the cytotoxicity of drug-loaded DNA nano-tetrahedrons to QBC939, RBE, and FRH-0201 of CC. The cells were inoculated in a 96-well plate, and different concentrations of doxorubicin and drug-loaded DNA nano-tetrahedrons (2, 4, 6, 8, and 10 μmol) were administrated when the cells grew to about 85. Then, the MTT solution was added at the 4th, 8th, 16th, 32nd, and 48th hour after the culture, and the formazan crystals were treated with dimethyl sulfoxide (DMSO) after 1 hour of reaction. The optical density (OD) was measured at 520 nm, and the cell survival rate was calculated.

TACE

The specific steps were as follows. The patient was placed in a supine position before treatment, treated with a conventional electrocardiograph (ECG) monitoring and oxygen inhalation, and sterilized on both sides of the groin. After the patient was anesthetized with 2% lidocaine locally, the 5F sheath was inserted with the Seldinger modified surgery, and then a 0.035-inch hydrophilic membrane guide wire was connected from the sheath to show the hepatic artery trend. The diluted chemotherapy drug was infused in the tumor blood vessel through the catheter. After the embolization was completed, the catheter and sheath were removed, the puncture point was compressed to stop the bleeding, and the wound was wrapped locally. The patient was required to stay in bed for at least 5 hours.

Biliary tract implantation based on I-125 radioactive particle stent loaded with nano-tetrahedral drugs

Before surgery, the number of particles needed should be evaluated based on the imaging data of the patient. The specific steps were as follows. The patient was required to lie supine on the operating table and locally anesthetized with 2% lidocaine. The puncture needle was inserted into the liver, and the occipital needle core was taken out. The contrast agent was injected into the bile duct for visualization with a syringe. The guide wire was fixed, and the puncture needle was taken out. The patient was incised a 5 cm opening for cholangiography. The guide wire was inserted into the 9F sheath and then sent to the biliary biopsy forceps through the sheath, so as to take several pieces of affected tissue in the narrowed bile duct. Then, the color monitoring catheter in the biliary puncture suit was sealed at the distal end, and the I-125 particle stent was sequentially inserted from the proximal end of the catheter with forceps. The particle chain stent was inserted into the biliary drainage tube through the guide wire and externally fixed with the biliary drainage tube.

Observation indicators

The TBIL, ALP, albumin (Alb), and liver function Child-Pugh scores of the patients in each group were recorded before the surgery (0 days), 7, 14, 21, and 30 days after the surgery. The long-term follow-up of patients was performed to record their five-year survival rate. The cell

survival rate of CC cell lines QBC939, RBE, and FRH-0201 were measured and recorded at different concentrations of doxorubicin and DNA nano-drug-loaded tetrahedrons and at different reaction times.

Statistical methods

The data processing was analyzed by SPSS19.0 version statistical software. The measurement data were expressed as mean ± standard deviation ($\bar{x} \pm s$), and the count data was given as a percentage (%). The indicators were compared pairwise with the one-way analysis of variance. The difference was statistically significant at $P< 0.05$.

Results

Optimization results of DNA nano-tetrahedral drug delivery system

Figure 1 shows the concentration of DNA tetrahedral at different initial concentrations of doxorubicin. It illustrated that the concentration of doxorubicin in the DNA nano-tetrahedron increased with the initial concentration of doxorubicin, and it tended to be stable at 150, 200, and 250 mol. Thus, the best initial concentration of doxorubicin could be determined as 200 μmol.

Figure 2 shows the concentration of DNA tetrahedral at different reaction times. It revealed that the amount of doxorubicin loaded in the DNA nano-tetrahedrons increased with the initial concentration of doxorubicin, but the increasing amount was lower at the 5th, 7th, and 9th hour and tended to be stable. Thus, it was obtained that the optimal reaction time should be 7 hours.

Cytotoxicity test results

Figure 3 shows the comparison of cell survival rates under different incubation times. It disclosed that the cell survival rates of the QBC939, RBE, and FRH-0201 showed downward trends with the extension of the incubation time. The cell survival rate at the 0th, 4th, 8th, and 16th hour decreased slowly, while that at the 32nd hour had dropped to about 50%, and it in the 48th hour had dropped to less than 30%. Therefore, after 16 hours of reaction, the toxicity of drug-loaded DNA nano-tetrahedrons to CC cells was greatly increased.

The comparison of cell survival rates at different concentrations was given in Figure 4 below. It indicated that the cell survival rate of QBC939, RBE, and FRH-0201 all showed a downward trend with the increase of the concentration of doxorubicin or drug-loaded DNA nano-tetrahedron. The cell survival rate decreased slowly when the concentration was 2, 4, 6, and 8 μmol, which had dropped to about 50% at 10 μmol, and had dropped below 35% at 12 μmol. Therefore, it was obtained that at

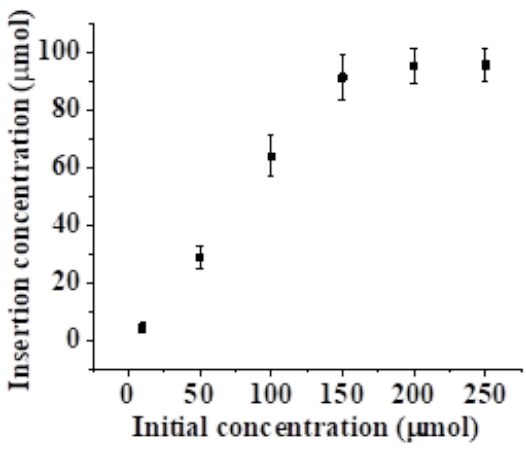

Figure 1. The concentration of DNA tetrahedral at different initial concentrations of doxorubicin.

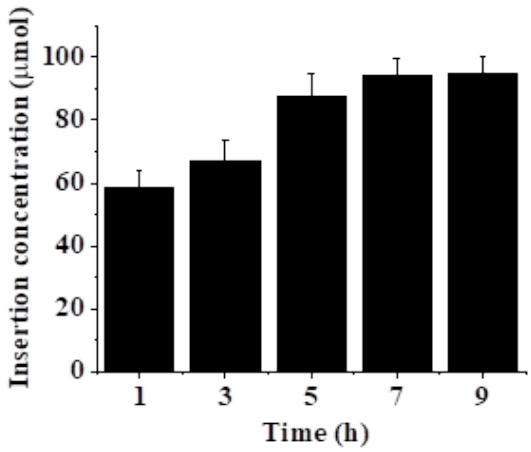

Figure 2. The concentration of DNA tetrahedral at different reaction times.

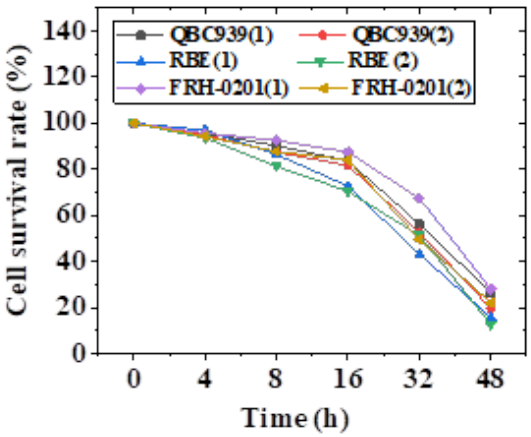

Figure 3. The comparison of cell survival rates under different incubation times. (QBC939(1), RBE(1), and FRH-0201(1) were the doxorubicin administration; while QBC939(2), RBE(2), and FRH-0201(2) were the drug-load nano-tetrahedron administration).

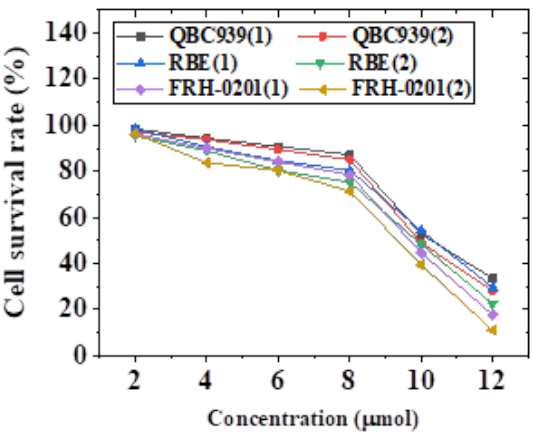

Figure 4. The comparison of cell survival rates at different concentrations. (QBC939(1), RBE(1), and FRH-0201(1) were the doxorubicin administration; while QBC939(2), RBE(2), and FRH-0201(2) were the drug-load nano-tetrahedron administration).

8 μmol of doxorubicin or drug-loaded DNA nano-tetrahedron showed less toxicity to CC cells.

Changes in TBIL and ALP levels of the three groups of patients before and after surgery

Figure 5 illustrates the changes in TBIL levels before and after the surgery in the three groups of patients. The preoperative TBIL and ALP levels of the three groups of patients were not statistically meaningful (P> 0.05); and the TBIL and ALP levels in the K1 group were greatly lower in contrast to the K2 and K3 groups in the 7th, 14th, 21st, and 30th days after surgery showing great differences (P< 0.05).

Figure 6 displayed the changes in ALP levels before and after the surgery of the three groups of patients. It illustrated that the preoperative ALP levels of the three groups of patients showed the trend of first decreasing and then increasing over time. The ALP level of patients in the K1 group was much lower than that of the patients in the K2 and K3 groups on the 7th, 14th, and 21st days after the surgery, showing meaningful differences (P< 0.05); and the ALP levels of the patients in the K1 group on the 0th and 30th day after the surgery were similar those in K2 and K3 groups, without statistical differences (P> 0.05).

Changes in ALB levels and liver function Child-Pugh scores of the three groups of patients before and after the surgery

The changes in ALB levels and liver function Child-Pugh scores of patients before and after the surgery were illustrated in Figure 7 and Figure 8, respectively. They revealed that the preoperative ALB level and the liver function Child-Pugh score of patients showed continuous decreasing trends over time in all groups; and those in the K1 group were not obviously different from those in the K2 and K3 groups on the 0th 7th, 14th, 21st, and 30th day after the surgery (P> 0.05).

Comparison of the 5-year survival rate of the three groups of patients

Figure 9 shows the comparison of the 5-year survival curves of the three groups of patients. The five-year survival rate of patients in the K1, K2, and K3 groups was 36.15 ±3.85%, 14.65 ±5.02%, and 16.78 ±4.31%, respectively, which indicated that the five-year survival rate of patients in group K1 was obviously higher than that of patients in group K2 and K3, with observable differences in statistics (P< 0.05).

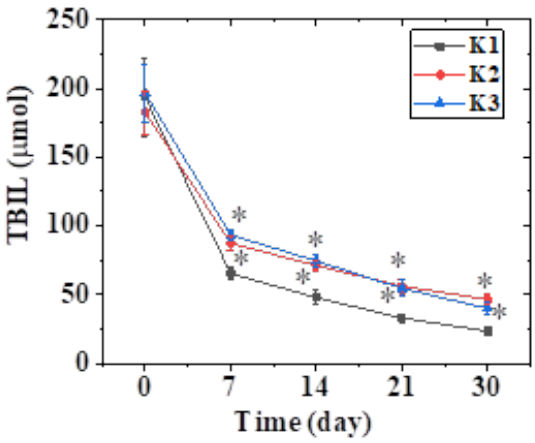

Figure 5. The changes in TBIL levels before and after the surgery in the three groups of patients. Note: * indicated that the difference was remarkable in contrast to K1 group (P < 0.05).

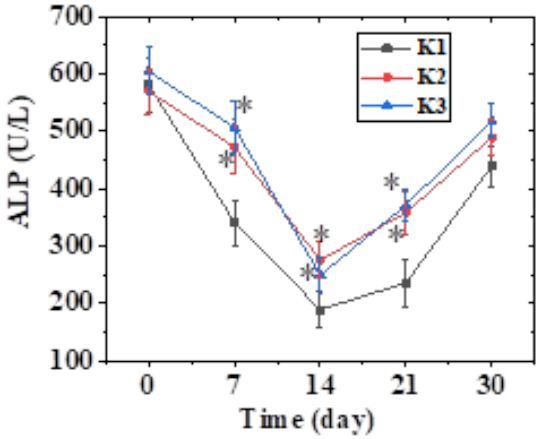

Figure 6. The changes in ALP levels before and after the surgery in the three groups of patients. Note: * indicated that the difference was remarkable in contrast to the K1 group (P< 0.05).

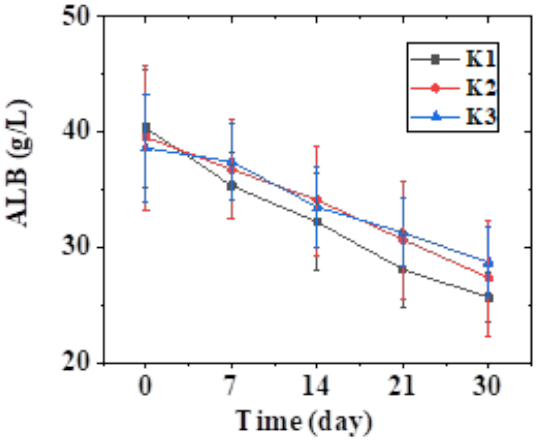

Figure 7. The changes in ALB levels before and after the surgery in the three groups of patients.

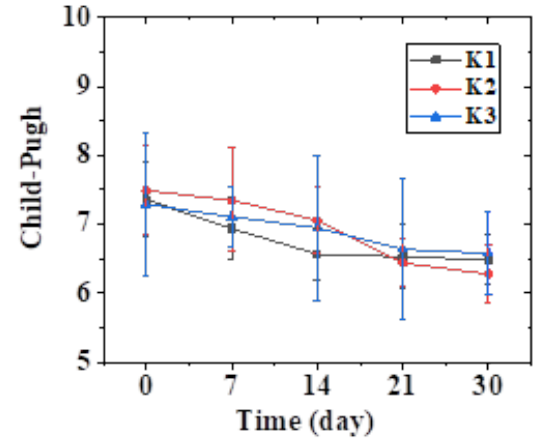

Figure 8. The changes in liver function Child-Pugh scores of patients before and after the surgery.

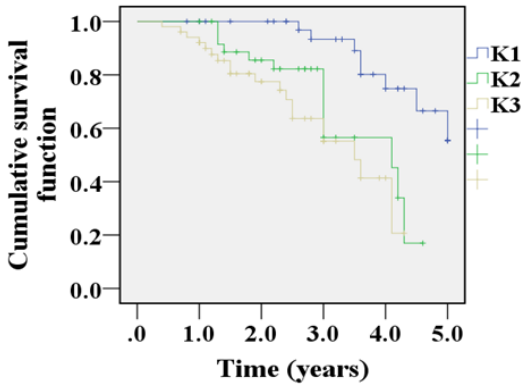

Figure 9. The comparison of the 5-year survival curves of the three groups of patients.

Discussion

As a relatively rare malignant tumor, extrahepatic CC has the characteristics of insidious onset, unobvious early symptoms, rapid progress, and poor prognosis of treatment. Therefore, most patients are already in the middle and late stages of the disease at the time of diagnosis, and the surgical treatment rate is decreased greatly (15). In recent years, the rapid development of nanotechnology has provided a more effective approach to the field of tumor diagnosis and treatment. Among them, the construction of nano-drug delivery systems has always been a key topic of research by scholars. It has great potential and can allow many drugs to target tumors in the body. The focus part can effectively treat tumor diseases. In addition, the development of structural DNA nanotechnology has enabled DNA to develop from traditional genetic material into a new type of material. Due to its good programmability and predictability, it has become one of the most promising nano-carriers (16). In this study, four DNA strands were adopted to construct the doxorubicin-loaded DNA nano-tetrahedrons. The preparation optimization and toxicity analysis revealed that the optimal initial concentration of doxorubicin-loaded DNA nano-tetrahedrons can be 200 μmol, and the optimal reaction time should be 7 hours. The cell survival rate of QBC939, RBE, and FRH-0201 decreased slowly at the 0th, 4th, 8^{th,} and 16th hour, had dropped below 30% at the 48th hour. Such results were similar to the results of Aliberti (2017) (17), indicating that the optimal incubation time used in the experiment should be 16 hours. The cell survival rate of QBC939, RBE, and FRH-0201 decreased slowly at 2, 4, 6, and 8 μmol, while the cell survival rate at 10 μmol had dropped to about 50%. It can be seen that 8 μmol doxorubicin or DNA nano-tetrahedron was the best concentration for the experiment (18).

The doxorubicin-loaded DNA nano-tetrahedrons were applied to the clinical treatment of 255 extrahepatic CC patients. The results showed that the TBIL levels of patients in the K1 group were much lower than those in the K2 and K3 groups at the 7th, 14th, 21st, and 30th day after the surgery (P< 0.05), which indicated that doxorubicin-loaded I-125 stent combined with TACE could reduce the TBIL level of the patient more effectively than a single treatment. The preoperative ALP levels of the three groups of patients showed the trends of the first decrease and then increase over time, and the ALP levels of patients in the K1 group were greatly lower in contrast to those in the K2 and K3 groups at the 7th, 14th, and 21st day after surgery (P< 0.05). Such results were different from the findings of Wang et al. (2020) (19), which may be due to the inconsistent time standard for drainage tube removal for the patient, which reduced the effect of stent combined with a drainage tube to a certain extent (20). It was found that the five-year survival rate of the K1 group was visibly higher in contrast to that of the K2 and K3 groups (P< 0.05), which indicated that the doxorubicin-loaded I-125 stent combined with TACE could effectively improve the five-year survival rate of patients and improve the prognosis.

The four DNA strands were applied to construct the doxorubicin-loaded DNA nano-tetrahedrons, the preparation protocol was optimized, and toxicity experiments were carried out. The prepared doxorubicin-loaded DNA nano-tetrahedrons were applied to the clinical treatment of 255 extrahepatic CC patients. The results showed that the optimal initial concentration of doxorubicin-loaded DNA nano-tetrahedrons for preparation of doxorubicin-loaded DNA nano-tetrahedrons could be 200 μmol, and the optimal reaction time could be 7 hours. The doxorubicin-loaded I-125 stent combined with TACE could effectively improve the five-year survival rate of patients and improve the prognosis. However, the sample size selected was too small to make statistics on subsequent anti-tumor treatment methods, CC classification, and other data. In the follow-up, it will consider increasing the sample size of patients and further analyze the factors affecting the effect of doxorubicin-loaded I-125 stent combined with TACE treatment. In conclusion, the results of this study could provide a theoretical basis for nano-drug therapy for CC patients.

Acknowledgments
Not applicable.

Interest conflict
The authors declare that they have no conflict of interest.

References

1. Currie BM, Soulen MC. Decision Making: Intra-arterial Therapies for Cholangiocarcinoma-TACE and TARE. Semin Intervent Radiol. 2017 Jun;34(2):92-100. doi: 10.1055/s-0037-1602591. Epub 2017 Jun 1. PMID: 28579676; PMCID: PMC5453778.
2. Hu Y, Hao M, Chen Q, Chen Z, Lin H. Comparison of the efficacy and safety among apatinib plus drug-eluting bead transarterial chemoembolization (TACE), apatinib plus conventional TACE and apatinib alone in advanced intrahepatic cholangiocarcinoma. Am J Transl Res. 2020 Oct 15;12(10):6584-6598. PMID: 33194055; PMCID: PMC7653562.
3. Schizas D, Mastoraki A, Routsi E, Papapanou M, Tsapralis D, Vassiliu P, Toutouzas K, Felekouras E. Combined hepatocellular-cholangiocarcinoma: An update on epidemiology, classification, diagnosis and management. Hepatobiliary Pancreat Dis Int. 2020 Dec;19(6):515-523. doi: 10.1016/j.hbpd.2020.07.004. Epub 2020 Jul 24. PMID: 32753331.
4. Kreidieh M, Zeidan YH, Shamseddine A. The Combination of Stereotactic Body Radiation Therapy and Immunotherapy in Primary Liver Tumors. J Oncol. 2019 Apr 28;2019:4304817. doi: 10.1155/2019/4304817. PMID: 31182960; PMCID: PMC6512065.
5. Liu JB, Chu KJ, Ling CC, Wu TM, Wang HM, Shi Y, Li ZZ, Wang JH, Wu ZJ, Jiang XQ, Wang GR, Ma YS, Fu D. Prognosis for

intrahepatic cholangiocarcinoma patients treated with postoperative adjuvant transcatheter hepatic artery chemoembolization. Curr Probl Cancer. 2020 Dec;44(6):100612. doi: 10.1016/j.currproblcancer.2020.100612. Epub 2020 May 28. PMID: 32517878.

6. Koch C, Franzke C, Bechstein WO, Schnitzbauer AA, Filmann N, Vogl T, Gruber-Rouh T, Zeuzem S, Waidmann O, Trojan J. Poor Prognosis of Advanced Cholangiocarcinoma: Real-World Data from a Tertiary Referral Center. Digestion. 2020;101(4):458-465. doi: 10.1159/000500894. Epub 2019 May 24. PMID: 31129660.
7. Wang L, Lin ZG, Ke Q, Lou JY, Zheng SG, Bi XY, Wang JM, Guo W, Li FY, Wang J, Zheng YM, Li JD, Cheng S, Zhou WP, Zeng YY. Adjuvant transarterial chemoembolization following radical resection for intrahepatic cholangiocarcinoma: A multi-center retrospective study. J Cancer. 2020 Apr 7;11(14):4115-4122. doi: 10.7150/jca.40358. PMID: 32368294; PMCID: PMC7196258.
8. Liu M, Khan A, Wang Z, Liu Y, Yang G, Deng Y, He N. Aptasensors for pesticide detection. Biosens Bioelectron. 2019 Apr 1;130:174-184. doi: 10.1016/j.bios.2019.01.006. Epub 2019 Jan 15. PMID: 30738246.
9. Huang R, He L, Xia Y, Xu H, Liu C, Xie H, Wang S, Peng L, Liu Y, Liu Y, He N, Li Z. A Sensitive Aptasensor Based on a Hemin/G-Quadruplex-Assisted Signal Amplification Strategy for Electrochemical Detection of Gastric Cancer Exosomes. Small. 2019 May;15(19):e1900735. doi: 10.1002/smll.201900735. Epub 2019 Apr 8. PMID: 30963720.
10. Pandey A, Pandey P, Aliyari Ghasabeh M, Najmi Varzaneh F, Shao N, Khoshpouri P, Zarghampour M, Fouladi DF, Liddell R, Kamel IR. Unresectable Intrahepatic Cholangiocarcinoma: Multiparametric MR Imaging to Predict Patient Survival. Radiology. 2018 Jul;288(1):109-117. doi: 10.1148/radiol.2018171593. Epub 2018 Mar 27. PMID: 29584595.
11. Ke Q, Lin N, Deng M, Wang L, Zeng Y, Liu J. The effect of adjuvant therapy for patients with intrahepatic cholangiocarcinoma after surgical resection: A systematic review and meta-analysis. PLoS One. 2020 Feb 21;15(2):e0229292. doi: 10.1371/journal.pone.0229292. PMID: 32084210; PMCID: PMC7034847.
12. Savic LJ, Chapiro J, Geschwind JH. Intra-arterial embolotherapy for intrahepatic cholangiocarcinoma: update and future prospects. Hepatobiliary Surg Nutr. 2017 Feb;6(1):7-21. doi: 10.21037/hbsn.2016.11.02. PMID: 28261591; PMCID: PMC5332218.
13. Goerg F, Zimmermann M, Bruners P, Neumann U, Luedde T, Kuhl C. Chemoembolization with Degradable Starch Microspheres for Treatment of Patients with Primary or Recurrent Unresectable, Locally Advanced Intrahepatic Cholangiocarcinoma: A Pilot Study. Cardiovasc Intervent Radiol. 2019 Dec;42(12):1709-1717. doi: 10.1007/s00270-019-02344-0. Epub 2019 Oct 2. PMID: 31578633.
14. Ge Y, Jeong S, Luo GJ, Ren YB, Zhang BH, Zhang YJ, Shen F, Cheng QB, Sui CJ, Wang HY, Xia Q, Chen L. Transarterial chemoembolization versus percutaneous microwave coagulation therapy for recurrent unresectable intrahepatic cholangiocarcinoma: Development of a prognostic nomogram. Hepatobiliary Pancreat Dis Int. 2020 Apr;19(2):138-146. doi: 10.1016/j.hbpd.2020.02.005. Epub 2020 Feb 21. PMID: 32139295.
15. Xiao Z, Yang G, Yan D, Li S, Chen Z, Li W, Wu Y, Chen H. Effects of diverse materials-based methods on DNA extraction for Clostridium difficle from stool samples. Materials Express. 2019 Aug 1;9(5):509-516.
16. Lai Y, Huang H, Xia Z, Li S, Deng Y, Liu X. A sandwich-type electrochemical immunosensor using polythionine/AuNPs nanocomposites as label for ultrasensitive detection of carcinoembryonic antigen. Materials Express. 2019 Aug 1;9(5):444-450.
17. Aliberti C, Carandina R, Sarti D, Pizzirani E, Ramondo G, Mulazzani L, Mattioli GM, Fiorentini G. Chemoembolization with Drug-eluting Microspheres Loaded with Doxorubicin for the Treatment of Cholangiocarcinoma. Anticancer Res. 2017 Apr;37(4):1859-1863. doi: 10.21873/anticanres.11522. PMID: 28373452.
18. Na SK, Choi GH, Lee HC, Shin YM, An J, Lee D, Shim JH, Kim KM, Lim YS, Chung YH, Lee YS. The effectiveness of transarterial chemoembolization in recurrent hepatocellular-cholangiocarcinoma after resection. PLoS One. 2018 Jun 7;13(6):e0198138. doi: 10.1371/journal.pone.0198138. PMID: 29879137; PMCID: PMC5991684.
19. Wang C, Meng F, Huang Y, He N, Chen Z. Design and Implementation of Polymerase Chain Reaction Device for Aptamers Selection of Tumor Cells. J Nanosci Nanotechnol. 2020 Mar 1;20(3):1332-1340. doi: 10.1166/jnn.2020.17356. PMID: 31492292.
20. Ma KW, Cheung TT, Leung B, She BWH, Chok KSH, Chan ACY, Dai WC, Lo CM. Adjuvant chemotherapy improves oncological outcomes of resectable intrahepatic cholangiocarcinoma: A meta-analysis. Medicine (Baltimore). 2019 Feb;98(5):e14013. doi: 10.1097/MD.0000000000014013. PMID: 30702559; PMCID: PMC6380775.